Experimental Study on Bond Behavior of GFRP Group Anchorage

Alireza Abolghasem, Hossein Azimi, Khaled Sennah, and Ekaterina Tropynina
Department of Civil Engineering, Ryerson University, Toronto, Canada

Abstract: Corrosion in steel reinforcement due to environmental effects is a major cause of deterioration problems in concrete bridges. The application of Glass Fibre Reinforced Polymer (GFRP) bars not only addresses this durability problem but also provides exceptionally high tensile strength along with high strength-to-weight ratio, and resistant to chemical attack. This paper presents an experimental investigation on the pull-out capacity of group of two or three GFRP bars embedded in concrete with various bar spacing and embedment length of 200 mm. The bar diameter used is 16 mm with ribbed surface. Two types of group actions were studied called double (group of two bars) or triple (group of three bars) with the horizontal nominal spacing of 150, 225, and 300 mm. For each case, five identical samples were constructed. Hence, the total of 30 samples were erected, 15 for double bars and 15 for triple bars. Four reinforced concrete slabs of 300 mm thickness were casted simultaneously and GFRP bars were pre-installed with 1 m clear spacing between double or triple bars to minimize any effect on each other. Results generally show that the smaller bar spacing generally reduces the failure bond stress caused by overlapping stress effect of the group of bars.

1. Introduction

Fiber reinforced polymer (FRP) reinforcement is proven to be one of the most effective alternative replacement for traditional steel reinforcement mainly to resolve durability problems such as corrosion associated with steel reinforcement. Glass-FRP (GFRP) bars have become one of the most popular types of FRP reinforcements because of their lower cost in the construction industry. Bridge deck slabs and parking garages are two of the most common places where GFRP reinforcements are being used especially in North America. These elements could be subjected to combinations of fatigue, traffic load, and freeze-thaw cycles. Considering the environmental conditions and different loading types that they are exposed to, the mechanical properties of the concrete, the FRP reinforcement and the bond between the FRP and concrete could be affected. For reinforced concrete structures that the stresses are continuously transferred between the bars and the concrete, not only the serviceability but also the ultimate limit state depends on the quality of bond between the two elements. Therefore, the bond between FRP bars to concrete elements subjected to thermal and mechanical loads might be critical design factor that needs to be investigated (Katz 2000 and Shahidi et al. 2006).

Different factors affect the bond behavior of FRP bars such as adhesion, bar diameter, bar surface pattern and shape. In addition, confining pressure surrounding the FRP bar due to volume change as a result of temperature and moisture variations and loading and environmental conditions, affect the bar resistance (Cosenza et al. 1997). Tepfers et al. (1998) and Galati et al. (2006) concluded that concentric placement of the bar in pullout tests reduces the bond strength from 30 to 50 percent compared with eccentric specimens with a concrete cover equal to twice bar diameter. Shahidi et al. (2006) studied the effects of sustained load on the bond of three types of bars: sand-coated GFRP with helical lugs, indented carbon (CFRP) bars and CFRP strands in pullout tests. They demonstrated that both CFRPs

show higher free-end slip under sustained load compared to steel bars. A comprehensive literature review on the pull-out capacity and mode of failures of bars embedded in concrete was addressed by Kim and Smith (2010).

However, no study in the literature was found to investigate the effect of group action on pull-out capacity of GFRP bars. When a bar is under tensile forces, the surrounding concrete is under stress. If the spacing between bars installed side by side in the concrete is too small, the stressed regions will have overlap which may eventually reduce the resulted pull-out capacity of the bar. This study presents the experimental results of the pull-out tests performed on group of two or three GFRP bars embedded in concrete with various bar spacing. The GFRP bars are pre-installed with an embedment length of 200 mm, bar diameter of 16 mm with ribbed surface. Two types of group actions studied are called double (group of two bars) or triple (group of three bars). The only parameter is the bar spacing to investigate the effect of group action.

2. Details of Experimental Program

2.1 Test specimens

Four concrete slabs of 30 m length, 1.35 m width and 300 mm depth were casted. The slabs were reinforced with top and bottom reinforcement made of 15M steel bars spaced at 300 mm each direction to include the confinement effect of internal reinforcement on the pull-out capacity of GFRP bars. An embedment length of 200 mm was chosen for the GFRP bars to be placed inside the concrete slab. A total of 30 group bars were embedded in the slabs. The nominal spacing between installed bars was selected 150, 225, and 300 mm for each specimen. Spacing of 300 mm was chosen since it is the maximum allowable mentioned in CHBDC (2006). Five identical samples were erected for each bar spacing. Distances between adjacent groups was maintained 1000 mm to accommodate the loading setup and remove any effect on each other. Therefore, the only parameter that differ in specimens was the bar spacing. The total of 30 samples were erected, 15 samples for double bars and 15 for triple bars.

2.2 Material properties

Concrete slabs were casted using ready mix concrete of minimum strength of 30 MPa on June 2011 and left for a year to consider the environmental effect on the samples. Concrete cylinders were tested to check the 28 day concrete strength. The concrete strengths resulted from cylinder tests were 35.7, 33.34, 28.31, 26.84 and 24.27 MPa. Thus, the average concrete strength was 29.69 MPa. The concrete slabs were casted in an open area site and were cured for 7 days following the concrete casting and was later left for one year after casting.

GFRP bars with a ribbed and coated surface were used in the current study (Schoeck, 2011). The matrix VEU resins of the GFRP bars were composed of modified vinyl ester with a maximum volume fraction of 25%. The fibre reinforcement was comprised of continuous ECR-glass fibres with a minimum volume fraction of 75%. 16 mm diameter bars were selected to be used in this study which is one of the most applicable sizes used in construction. They have a core diameter of 16 mm, exterior diameter of 18 mm and the nominal area of 201 mm^2. Table 1 presents the material properties of the used GFRP bars. For all bar diameters, tensile rupture occurs at stresses as high as 1,000 MPa.

Table 1. Material properties of GFRP bars

Properties	Terms	Values
Ultimate tensile strength	F_u	1188 MPa
Modulus of elasticity	E_f	64 GPa
Ultimate elongation	ε_u	2.61%
Bond stress	τ_f	12.2 MPa
Transverse shear strength	t	150 MPa

3. Test Setup and Procedure

Two test setups were designed and assembled considering ASTM (2010) requirements to be used to test all the pre-installed GFRP anchorage samples. The main parameter that needs to be considered is the distance between support of the test setup and the bars being tested, which should be minimum $2L_e$ as specified by ASTM (2010), where L_e is the embedment depth of the GFRP bars. This was also reported by Ahmed et al. (2008) that a minimum of $2L_e$ is required to minimize any effect on pull-out capacity of post-installed GFRP bars. For the studied samples, the embedment length is constant that equals to 200 mm. Therefore, the clear spacing between support of the test setup and GFRP bars was considered minimum 400 mm in all specimens, where majority of test setups have spacing even more than 400 mm.

The developed test setups have two sets of I-shaped steel beams, 8 hollow steel sections (HSS), three load cells and grips to hold the bar as shown in Figures 1(a) and 1(b) for double and triple test setups, respectively. The length of I-beam is chosen to satisfy the aforementioned minimum clearance requirement for test equipment supports. The load was transferred from the hydraulic jack to the grips at the end of the GFRP bars. The load cells are placed between the grips and HSS sections to record the magnitude of the applied load on each bar. Hydraulic jacks and the load cells were connected to data acquisition system to continuously record the experimental results up to the failure of GFRP anchors. Figures 1(a) and 1(b) demonstrate the details of the developed test setups.
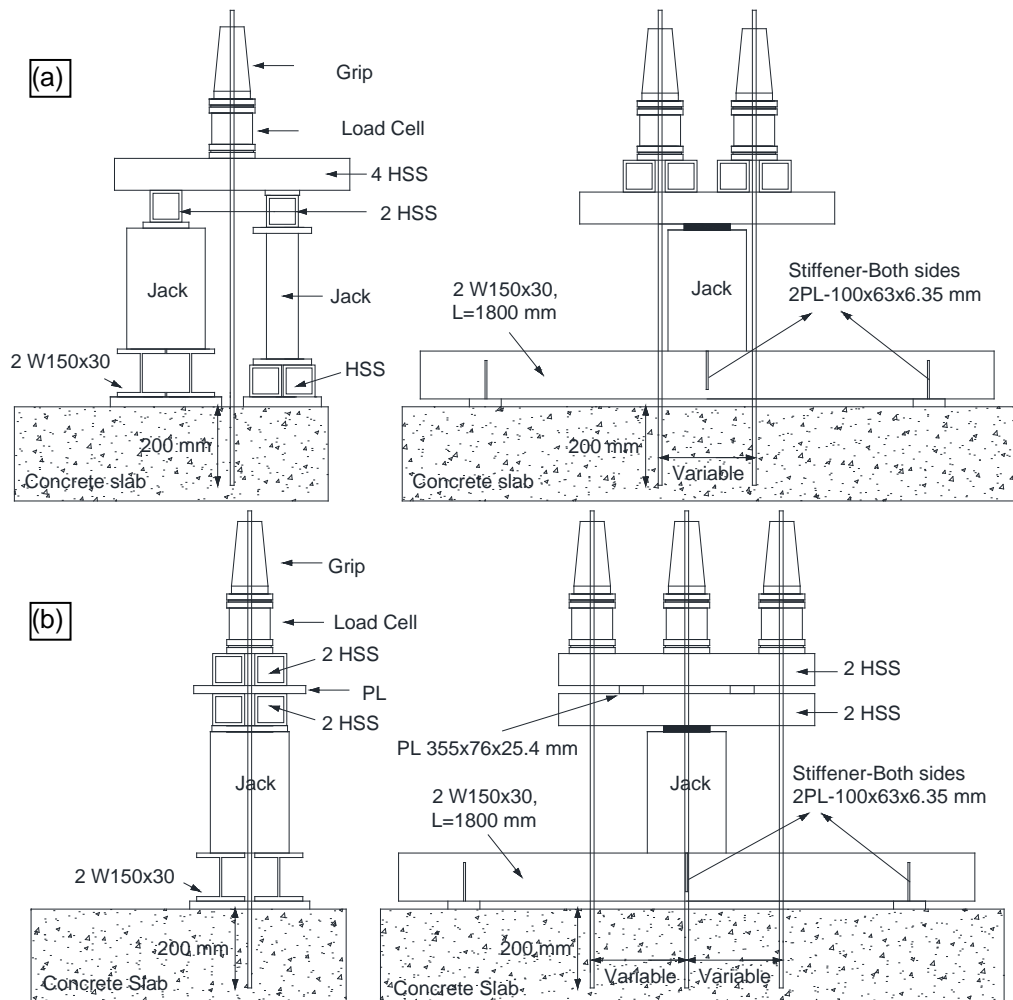

Figure 1. Test setup for (a) double bars, (b) triple bars

For the test setup of the triple bars, the plate between two rows of HSS sections shown in Figure 1(b) are placed such that the applied load from jack being transferred equally between three bars. For each specimen, the clear spacing between bars was measured on site and then location of plates was calculated using a simple formula developed for this purpose. In addition, two hydraulic jacks are used for the test setup of the double bars. The load of two jacks was simultaneously increased by two separated manual pumps to avoid rotation of HSS sections above the jacks preventing the tested bars from tilting during the test. For safety purposes, fastening straps were used to hold the members together after the GFRP anchor failure as shown in Figure 2. In both double and triple bars, after the failure of the first bar, the experiment was continued until failure of all bars.

Figure 2. Front view of the test setup for double bars

4. Experimental Results and Discussion

After performing the pullout test, four different modes of failure were observed as presented in Table 2, that are concrete cone failure (presented as type A), small concrete cone and GFRP/Concrete interface failure (type B), deep concrete cone and GFRP/concrete interface failure (type C) and GFRP bar rupture (type D).

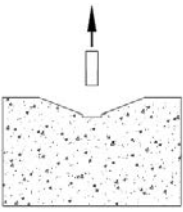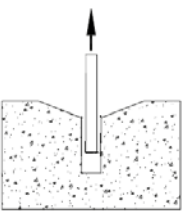Table 2. Observed pull-out modes of failure
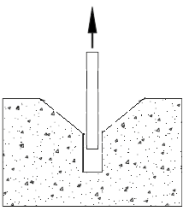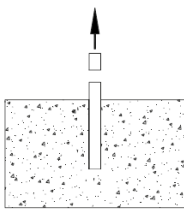
Type A	Type B	Type C	Type D
concrete cone failure	Small concrete cone and GFRP/concrete interface failure	Deep concrete cone and GFRP/concrete interface failure	GFRP bar rupture

.

Figure 3. Sample of mode of failures observed in specimen D-N5-150S-S3

Figure 3 shows an example of failure patterns observed during the pull-out tests illustrating the overlapping of concrete cone failures in double bar groups with 150 mm bar spacing. The left bar in Figure 4 demonstrated type C failure shown in Table 2 while the right bar had the failure of type B

The test results showing the failure load and stress, bond stress, average and maximum bond stress in addition to the modes of failure are presented in Table 3. The test samples were mainly divided into two series based on the number of GFRP bars in the group (double and triple). In addition, the test specimens in each group included three different bar spacing of 150, 225 and 300 mm. Each sample is designated by a set of symbols and numbers to be identified. As an example, for T-N5-150S-S1, the first letter T denotes triple bar sample, N5 denotes the bar number (which is number 5 in this case that has a 16mm diameter), 150S represents the spacing which is 150 mm in this case and finally S1 demonstrates the sample number (sample 1). For double bar samples, the same designation is used except the first letter which is D denoting double bar samples.

Third column of Table 3 presents the bar number for each individual bar in the group. There are 3 bar numbers for triple bar groups and 2 bar numbers for double bar groups. In addition, failure loads are given in Table 3 which are the loads measured by the load-cells and recorded by data acquisition system. the fifth column of Table 3 shows the stress in each bar which is calculated based on the measured failure load divided by the bar cross-sectional area, that is comparable with ultimate tensile strength of 1000 MPa mentioned in Table 1. The cross sectional area was calculated by the nominal diameter of 16 mm mentioned in Table 1. Bond stress, on the other hand, was calculated using Equation 1 by dividing the measured failure load by the perimeter area of the GFRP bar surrounded by concrete (embedment depth times the perimeter of the bar).

$$[1] \ \tau = \frac{F_u}{\pi d_b \, h_e}$$

Where, τ =average bond stress (MPa), F_u= failure load (N), d_b= bar diameter (mm) and h_e= embedment depth (mm). The maximum bond stress is also given in Table 3 demonstrating the maximum calculated bond stress in each sample among the three bars in case of triple bars or two bars for double bars for which the bar failure occurred. Consequently, the average bond stress is calculated from the aforementioned maximum bond stresses. The average bond stress is reported as a ± s where a is the mean value and s is the standard deviation. Finally, the type of failure is shown in the last column of the table by letters A, B, C and D that are defined in Table 2. The results presented in Table 3 are also shown as a graph in Figure 4, which provides a visual representation of the results. The bond stress calculated for each bar subjected to pull-out test is presented in this graph versus bar spacing for both double and triple groups considering three different spacing of bars. It could be concluded from this graph that, in general, increasing the bar spacing will augment the average bond stress. In other words, with the increase in the bar spacing in either the triple or double bar groups, more bond stress is carried, and consequently more pull-out failure force will be resulted.

Table 3. Experimental results of double and triple bars

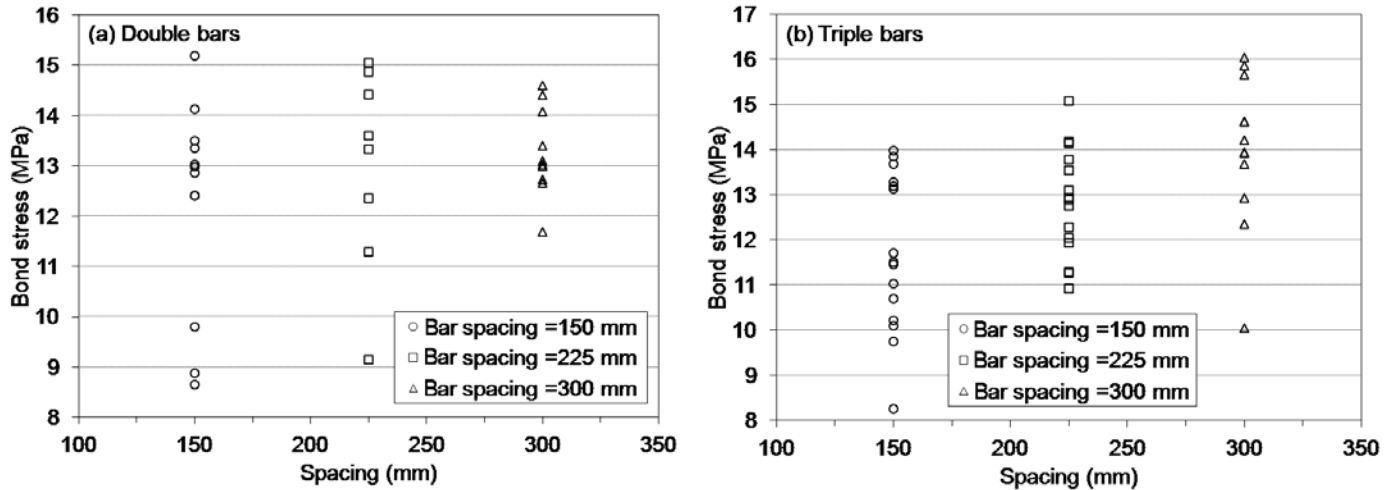| Setup type (1)	Designation (2)	Bar # (3)	Failure load (Kn) (4)	Stress (MPa) (5)	Bond stress (MPa) (6)	Maximum bond stress (MPa) (7)	Average bond stress (MPa) (8)	Type of mode of failure (9)
Triple bars	T-N5-150S-S1	1	115.8	575.9	11.5	11.51		A
		2	102.8	511.2	10.2			A
		3	101.3	503.7	10.7			A
	T-N5-150S-S2	1	132.0	656.7	13.1	13.13		B
		2	117.8	585.8	11.7			B
		3	98.0	487.6	9.8			B
	T-N5-150S-S3	1	140.5	699.0	14.0	13.98	13.23±1.01	B
		2	133.5	664.2	13.3			B
		3	101.5	505.0	10.1			B
	T-N5-150S-S4	1	115.3	573.4	11.5	13.85		C
		2	139.3	692.8	13.9			B
		3	83.0	412.9	8.3			B
	T-N5-150S-S5	1	132.6	659.9	13.2	13.68		C
		2	137.5	684.2	13.7			B
		3	110.9	551.8	11.0			B
	T-N5-225S-S1	1	120.1	597.6	11.9	11.94		C
		2	113.4	563.9	11.3			B
		3	113.5	564.7	11.3			B
	T-N5-225S-S2	1	109.9	546.6	10.9	12.76		C
		2	123.4	614.1	12.3			B
		3	128.3	638.4	12.8			C
	T-N5-225S-S3	1	121.1	602.6	12.1	13.54	13.49±1.21	C
		2	130.0	646.6	12.9			B
		3	136.1	677.1	13.5			C
	T-N5-225S-S4	1	142.1	707.2	14.1	14.14		C
		2	138.5	689.3	13.8			B
		3	131.7	655.2	13.1			B
	T-N5-225S-S5	1	129.6	644.9	12.9	15.08		B
		2	151.6	754.4	15.1			B
		3	142.6	709.5	14.2			B
	T-N5-300S-S1	1	138.1	687.3	13.9	14.62		C
		2	130.0	646.6	12.9			B
		3	147.0	731.4	14.6			C
	T-N5-300S-S2	1	124.1	617.5	12.4	16.04		B
		2	101.0	502.5	10.1			C
		3	161.3	802.5	16.0			B
	T-N5-300S-S3	1	157.4	783.1	15.7	15.66	15.55±0.64	B
		2	140.1	696.8	13.9			C
		3	142.9	710.7	14.2			B
	T-N5-300S-S4	1	159.4	793.1	15.9	15.86		B
		2	137.5	684.2	13.7			C
		3	147.0	731.4	14.6			B
Double bars	D-N5-150S-S1	1	124.8	620.6	12.4	14.13		B
		2	142.0	706.5	14.1			B
	D-N5-150S-S2	1	131.0	651.7	13.0	13.03		C
		2	129.3	643.0	12.9			C
	D-N5-150S-S3	1	87.0	432.8	8.7	13.35		C
		2	134.3	667.9	13.4			B
	D-N5-150S-S4	1	135.8	675.4	13.5	15.19	13.52±1.00	B
		2	152.8	760.0	15.2			B
	D-N5-150S-S5	1	89.3	444.0	8.9	12.98		B
		2	130.5	649.3	13.0			C
	D-N5-150S-S6	1	98.5	490.0	9.8	12.41		B
		2	124.8	620.6	12.4			C
	D-N5-225S-S1	1	92.0	457.7	9.2	11.29		B
		2	113.5	564.7	11.3			B
	D-N5-225S-S2	1	136.8	680.3	13.6	14.87		B
		2	149.5	743.8	14.9			C
	D-N5-225S-S3	1	124.3	618.2	12.4	14.42	13.91±1.77	B
		2	145.0	721.4	14.4			C
	D-N5-225S-S4	1	134.0	666.7	13.3	15.05		B
		2	151.3	752.5	15.1			B
	D-N5-300S-S1	1	131.0	651.7	13.0	14.08		C
		2	141.5	704.0	14.1			B
	D-N5-300S-S2	1	117.5	584.6	11.7	14.6		B
		2	146.8	730.1	14.6			B
	D-N5-300S-S3	1	128.0	636.8	12.7	12.73	13.78±0.83	B
		2	127.3	633.1	12.7			B
	D-N5-300S-S4	1	144.9	720.8	14.4	14.41		C
		2	134.8	670.4	13.4			D
	D-N5-300S-S5	1	130.6	649.9	13.0	13.1		B
		2	131.7	655.4	13.1			B

Figure 4. Bond stress vs. bar spacing for all double and triple bar groups

Figure 5, on the other hand, presents the influence of bar spacing on average bond stress of double and triple bar groups more clearly. Figure 5(a) shows the average bond stress of all bars that was recorded during the experiment in each category, while Figure 5(b) presents the average of the maximum bond stress measured in each sample that are those mentioned in column 8 of Table 3. Figure 5 shows that for both double and triple bar groups, increasing the spacing between the bars will usually lead to an increase in average bond stress. It also demonstrates that double bar group is able to carry more bond stress compared to triple group when spacing is 150 and 225 mm, while by increasing the spacing from 225 to 300 mm, triple bar group seems to be able to carry more bond stress in average compared to double bar group.

Both Figures 5(a) and 5(b) confirm the fact that the effect of bar spacing was more significant in triple bars. In triple bar specimens, the middle bar receives the overlapping stress effect from two side bars, while the side bars or the two bars used in double bar groups receive only the effect of one adjacent bar. Therefore, from theoretical point of view, it is expected to have more effect of bar spacing on triple bars compared to double bars, which is shown in Figures 5(a) and 5(b) for the spacing of 150 mm and 225 mm. Bar spacing of 300 mm showed no overlapping failure during experiment either in double or triple bars. In addition, as shown in Figure 5 for triple bars, a clear increase in bond stress is observed for bars with 300 mm spacing confirming less overlapping effect on such bars.
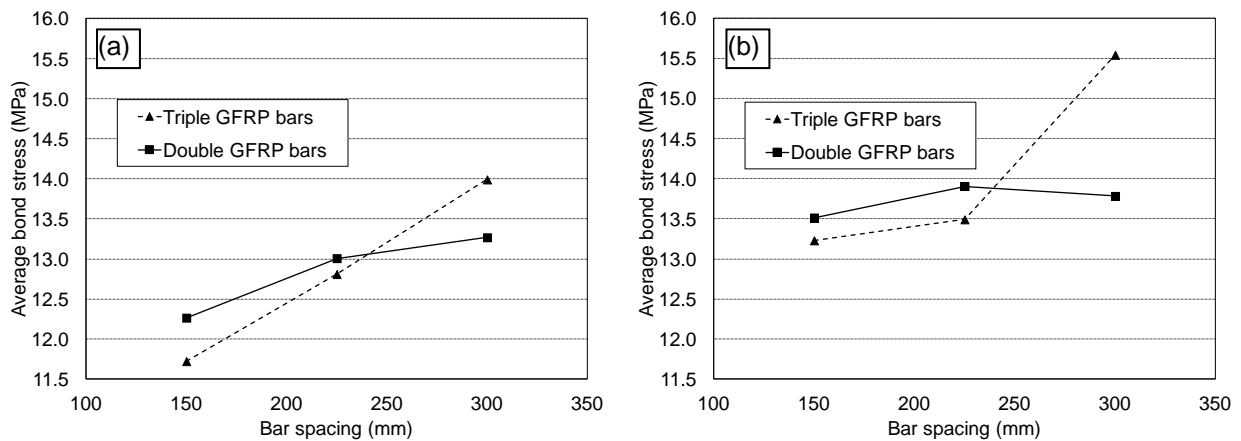

Figure 5. Average bond stress for triple and double bar groups: (a) average bond stress of all bars, (b) average bond stress of maximum force in each sample

One of the major types of failure is called concrete cone failure which happens when the failure surface forms in the shape of a concrete cone during the pull-out test shown as type A failure in Table 2. Another mode of failure, shown as type C in Table 2, is the combined concrete cone and bond failure. Table 4 presents three representative formulas used for calculating the concrete cone failure load for steel rebars suggested by ACI (1985), Eligehausen et al. (2006) and ACI (2005). The fourth equation is presented by Kim and Smith (2010) for concrete cone pull-out resistance of FRP bar anchors. The notation used in Table 4 for the concrete cone failure is N_{cc} and for combined cone-bond failure is N_{cb}. The bonded interface resistance model, N_{cb}, assumes the failure surface to be adjacent to the surface of the embedded portion of the bar at the bar-concrete interface. Important parameters for this type of failure are the bond stress of the interface and the failure surface. The last two equations presented in Table 4 are the pull out resistance based on bond failure mode for steel bar (Cook and Kunz, 2001) and combined bond-cone failure for FRP bars (Kim and Smith, 2010).

In Table 4, f'_c is the compressive strength of the concrete, A_c is projected area of a single anchor, h_{ef} is the effective embedment depth, d is the bar diameter, and d_h represents the diameter of anchor head which is the same as d in this paper, since no headed GFRP bars were used. A parameter k is also used in Table 4, which is an empirical coefficient that largely depends on the anchor type.

Failure load is calculated in Table 4 based on each suggested formula and average bond stress is also presented in the last column. Calculation of the average bond stress is done in accordance with Equation 1 after the calculation of failure loads and considering the bar diameter of 16 mm and embedment depth of 200 mm used in this paper.

Table 4. Selected existing analytical models for calculating failure load based on the type of failure

Reference	Relationship	Failure load (Kn)	Average bond stress (MPa)
ACI (1985)	$N_{cc}= 0.33\sqrt{f'_c}\,A_c$ $A_c=\pi h_{ef}(h_{ef}+d_h)$	245.3	24.4
Eligehausen et al. (2006)	$N_{cc}= k\,h_{ef}^{1.5}\sqrt{f'_c}$, $k=16.8$	260.3	25.9
ACI (2005)	$N_{cc}=k\,h_{ef}^{1.5}\sqrt{f'_c}$, $k=10$	154.9	15.4
Kim and Smith (2010)	$N_{cc}=9.68\,h_{ef}^{1.5}\sqrt{f'_c}$	149.9	14.9
Cook and Kunz (2001)	$N_{cb}=\tau\pi d h_{ef}$, $\tau=15.4$	154.8	15.4
Kim and Smith (2010)	$N_{cb}=9.07\pi d h_{ef}$, $f'_c>20$ MPa	91.2	9.1

Comparing the concrete cone resistance calculated based on the first two relationships in Table 4 with the numbers derived from the experimental works presented in Table 3 shows that the first two relationships give much higher value for pull-out capacity than those obtained experimentally. When the bar spacing is 300 mm, the pull-out capacity of the group approaches the numbers calculated from ACI (2005) and Kim and Smith (2010) for cone failure and Cook and Kunz (2001) for bond failure. Since the formulas presented by Kim and Smith (2010) were developed for FRP bar anchors, they provide results that could be used as upper bound and lower bound for experimental results obtained in this paper. However, the effect of bar spacing should be added to such formulas. However, more research is required with various embedment lengths and bar spacing in order to propose correction factors to such equations.

5. Conclusions

An experimental investigation on the pull-out capacity of group of two or three GFRP bars embedded in concrete with various bar spacing and embedment length of 200 mm was performed. 16 mm bars with ribbed surface were used. Two types of group actions (double and triple bars) were studied with the horizontal nominal spacing of 150, 225, and 300 mm. For each case, five identical samples were tested.

Four reinforced concrete slabs of 300 mm thickness were casted simultaneously and GFRP bars were pre-installed that was left in open area for one year to include one-year cycle of environmental effects. Experimental results showed that, in general, increasing the bar spacing increases the bond stress which implies that the group can carry more tensile loads. This could be rationalized by considering the influence of the bars on each other when placed as a group. The stress distributed in the concrete due to the pull-out load could have overlap if bars are closely placed in the concrete. As expected, experimental results demonstrated that double bar groups can carry more bond stress compared to triple group at spacing of 150 and 225 mm, since the middle bar of triple bar groups is affected by two side bars, while in double bar groups each bar is affected by only one adjacent bar. Moreover, by increasing the spacing to 300 mm, the overlapping effect decreases and triple bar groups pull-out capacity becomes higher than those obtained for double group bars. The effect of overlapping stresses was clearly observed in several specimens with 150 mm bar spacing where conic failure of bars overlapped. Experimental results showed that the effect of bar spacing should be considered in the formulas of pull-out failure load; however, more research is required with various embedment lengths and bar spacing in order to generalize the results.

Acknowledgement

References

Ahmed, E.A., El-Salakawy, E.F., and Benmokrane, B. 2008. Tensile capacity of GFRP postinstalled adhesive anchors in concrete. *Journal of Composites for Construction, ASCE.* 12(6): 596–607.

American Concrete Institute (ACI). 1985. *Code requirements for nuclear safety related concrete structures.* ACI 349-85, Detroit.

American Concrete Institute (ACI). 2005. *Building code requirements for structural concrete and commentary*. ACI 318M-05, Detroit.

ASTM. (2010). *Standard test methods for strength of anchors in concrete elements*. E488/E488M-10, West Conshohocken, PA.

CAN/CSA-S6 2006. *Canadian highway bridge design code (CHBDC)*. Canadian Standards Association, Mississauga, Ontario, Canada.

Cook, R.A. and Kunz, R.C. 2001. Factors influencing bond strength of adhesive anchors. *ACI Structural Journal*. 98(1): 76–86.

Cosenza, E., Manfredi, G., and Realfonzo, R. 1997. Behaviour and modeling of bond of FRP rebars to concrete. *Journal of Composites for Construction, ASCE*. 1(2): 40–51.

Eligehausen, R., Cook, R.A., and Appl. J. 2006. Behaviour and design of adhesive bonded anchors. *ACI Structural Journal*. 103(6): 822–831.

Galati, N., Nanni, A., Dharani, L., Focacci, F., and Aiello, A. 2006. Thermal effects on bond between FRP rebars and concrete. *Composites Part A: Applied Science and Manufacturing.* 37(8): 1223–1230.

Katz, A. 2000. Bond to concrete of FRP rebars after cyclic loading. *ASCE Journal of Composites for Construction*. 4(3): 137–144.

Kim, S.J., and Smith, S.T. 2010. Pullout strength models for FRP anchors in uncracked concrete. *ASCE Journal of Composites for Construction*. 14(4): 406-414.

Shahidi, F., Wegner, L., and Sparting, B. 2006. Investigation of bond between fibre-reinforced polymer bars and concrete under sustained loads. *Canadian Journal of Civil Engineering*: 33: 1426–1437.

Schoeck. (2011). *Schöck ComBAR Technical Information*. Schoeck Canada Inc.

Tepfers, R., Hedlund, G., and Rosinski, B. 1998. Pull-out and tensile reinforcement splice tests with GFRP bars. *2nd International Conference on Composite in Infrastructure (ICCI)*, 37–51.